Portugaliae Electrochimica Acta 2014, 32(5), 337-354

DOI: 10.4152/pea.201405337

PORTUGALIAE ELECTROCHIMICA ACTA
ISSN 1647-1571

Inhibition Effect of 2-Amino, 5-Ethyl- 1, 3, 4 Thiadiazole on the Corrosion of Austenitic Stainless Steel Type 304 in Dilute Sulphuric Acid

R.T. Loto,[a,b,*] C.A. Loto,[a,b] A.P.I. Popoola,[b] T.I. Fedotova[b]

[a]*Department of Mechanical Engineering, Covenant University, Ota, Ogun State, Nigeria*
[b]*Department of Chemical, Metallurgical and Materials Engineering, Tshwane University of Technology, Pretoria, South Africa*

Received 2 March 2014; accepted 28 October 2014

Abstract

The inhibition effect of 2- amino, 5- ethyl- 1, 3, 4 thiadiazole (TTD) compound on the corrosion of type 304 stainless steel in 3 M H_2SO_4 test solution was investigated using potentiodynamic polarization, weight loss techniques and open circuit potential measurements. Results showed TTD to be very effective with an average inhibition efficiency of 98% from weight loss analysis and 87% from polarization test. Data from open circuit potential measurement are well within passivation potentials at specific concentrations of TTD. Scanning electron microscopy showed the effect of the inhibiting compound on the surface topography of the steel, while X - ray diffractometry determined the phase compounds formed on the surface due to inhibitor adhesion. Adsorption of the compound was determined to obey the Langmuir isotherm model. Thermodynamic calculations showed the inhibition process occurred through chemisorption mechanism and results from statistical analysis revealed the overwhelming influence of inhibitor concentration over exposure time on the inhibition performance of the compound.

Keywords: corrosion; inhibitor; sulphuric acid; adsorption; Langmuir; steel.

Introduction

Corrosion is a major cause of concern in the industrial application of ferrous alloys due to the enormous cost involved in damages due to material deterioration, maintenance and corrosion control as a result of the aggressive nature of industrial environments and their interaction with the surface of

* Corresponding author. E-mail address: tolu.loto@gmail.com

equipments, machinery and devices; such as in acid pickling of steel, chemical cleaning and processing, ore production, chemical processing plants, automobile industries, oil well acidification, etc. [1, 2]. This necessitates attention from researchers worldwide for novel, cost effective, and environmentally friendly corrosion prevention techniques. Corrosion inhibitors are extensively applied to minimize the corrosion of metallic alloys; however, most inhibitors are hazardous and expensive [3-5]. Organic compounds containing oxygen, sulfur, nitrogen atoms, and multiple bonds in the molecules are widely used as acid inhibitors. A significant number of these compounds have been used as corrosion inhibitors in the past with satisfactory results, such as phosphonic acids, nitrite, polyacrylamide and phosphates [6-9]. Just recently investigation has been reached on the use of pharmaceutical drugs as inhibitors due to their innoxious attrinute such as Cefatrexyl, Cefatrexyl-Ciprofloxacin, Cefatrexyl-Ofloxacin, Cefatrexyl and Tacrine [10-12]. The inhibition performance of organic compounds is subject to their adsorption strength on metallic surfaces replacing molecules of water [13]. The adsorption is influenced by the electronic structure of the molecules of the organic compound, aromaticity, electron density, steric factors, molecular weight and functional groups [14, 15]. This research aims to investigate the inhibition effect of 2-amino, 5 ethyl, 1, 3, 4 thiadiazole, an inexpensive and non-toxic chemical compound used commercially for organic synthesis on Type 304 stainless steel corrosion in sulphuric acid to evaluate its inhibition efficiency and corrosion inhibition properties.

Experimental procedure

Material

Type 304 stainless steel was the test sample for the research investigation. Energy dispersive spectrometer analysis from the Electrochemical and Materials Characterization Research Laboratory, Department of Chemical and Metallurgical and Materials Engineering, Tshwane University of Technology, South Africa, with average nominal composition is shown in Table 1:

Table 1. Energy dispersive spectrometer analysis of ASS before immersion.

C	O	Si	S	Cr	Mn	Fe	Ni	TOTALS
0.07	0.76	0.73	0.8	18.13	1.17	70.15	8.09	99.97

The material is cylindrical with a diameter of 18 mm.

Inhibitor

2-amino, 5-ethyl- 1, 3, 4-thiadiazole (TTD), a transparent and whitish solid flakes obtained from SMM Instruments, South Africa, is the organic compound used as inhibitor. The structural formula of TTD is shown in Fig. 1. It has a molecular formula of C_4 H_7 N_3 S, with a molar mass of 129.18 $gmol^{-1}$. TTD was analytically prepared in percentage concentrations of 0.125%, 0.25%, 0.375%, 0.5%, 0.625% and 0.75%, respectively.

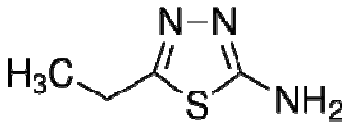

Figure 1. Chemical structure of 2-amino, 5-ethyl, 1, 3, 4-thiadiazole (TTD).

Test solution

3 M sulphuric acid (H_2SO_4) and 3.5% recrystallised sodium chloride (NaCl) were the simulated corrosive environment used for the research.

Preparation of test specimens

The stainless steel with a cylindrical dimension of 18 mm diameter was machined into samples ranging between 17.8 mm and 18.8 mm in length. A 3 mm hole was drilled at the centre for suspension of the sample in the corrosive media. The surface ends of the samples were metallographically prepared with silicon carbide sandpapers with grits up to 1000 before being polished with diamond paste to 1.0 μm and cleansed with distilled water.

Weight-loss experiments

Weighted test species were fully and separately immersed in 200 mL of the test media at specific concentrations of the TTD for 360 h at ambient temperature of 25 ^{o}C. Each of the test specimens was taken out every 72 h, washed with distilled water, rinsed with acetone, dried and re-weighed. Plots of weight-loss (mg), corrosion rate (mm/y) and percentage inhibition efficiency (*%IE*) versus exposure time (h) (Figs. 2, 3 and 4) for the test media and those of percentage inhibition efficiency (*%IE*) (calculated) versus percentage TTD concentration (Fig. 5) were deduced from Table 2.

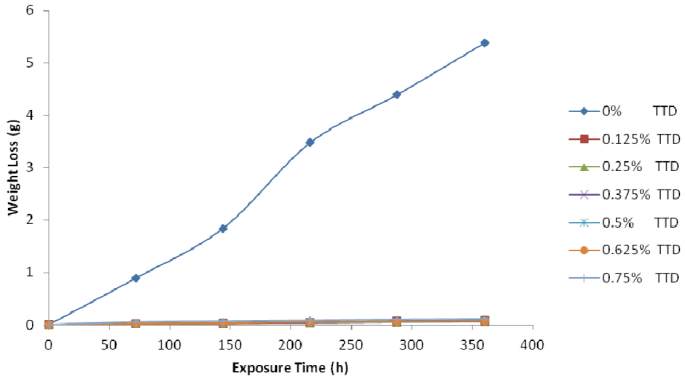

Figure 2. Variation of weight-loss with exposure time for samples (A – G) in 3 M H_2SO_4.

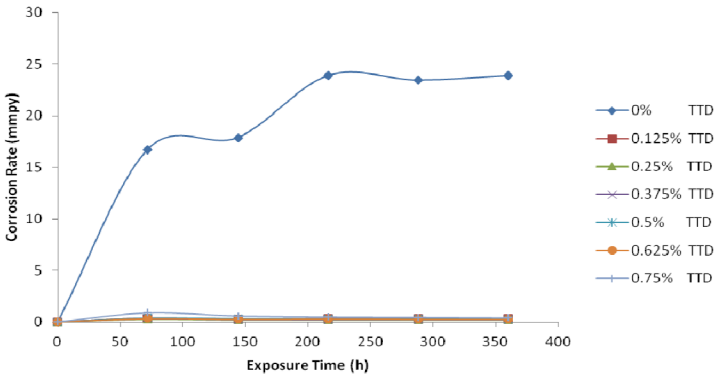

Figure 3. Effect of percentage concentration of TTD on the corrosion rate of austenitic stainless steel in 3 M H_2SO_4.

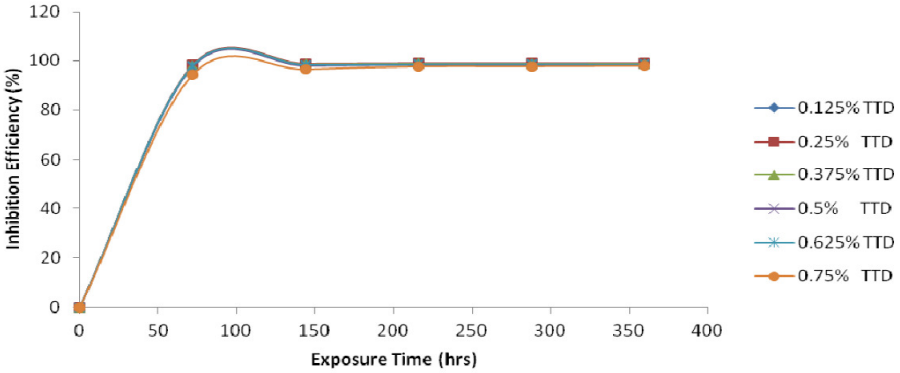

Figure 4. Plot of inhibition efficiencies of samples (A-G) in 3 M H_2SO_4 during the exposure period.

The corrosion rate (R) is calculated from equation 1:

$$R = (87.6W/DAT) \quad (1)$$

where W is the weight loss (mg), D is the density in (g/cm^3), A is the area in cm^2, and T is the time of exposure in hours. The $\%IE$ was calculated from the relationship in equation 2.

$$\%IE = (W1 - W2/W1) \times 100 \quad (2)$$

where W_1 and W_2 are the weight loss of steel in with and without specific concentrations of TTD. The $\%IE$ was calculated every 72 h during throughout the research investigation. The surface coverage is calculated as shown below:

$$\theta = (1 - W2/W1) \quad (3)$$

θ is the amount of TTD adsorbed onto the steel surface.

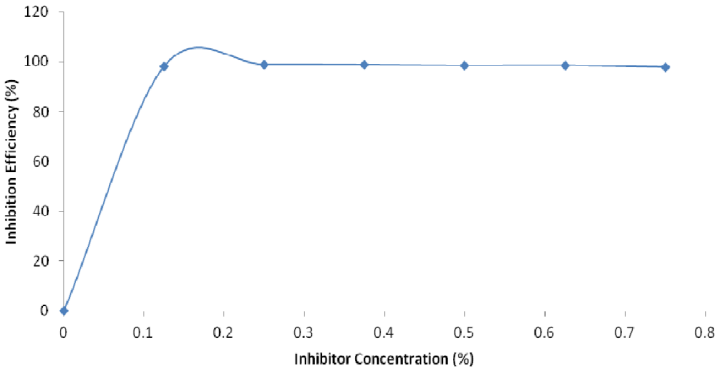

Figure 5. Variation of the percentage of the inhibition efficiency of TTD with inhibitor concentration in 3 M H_2SO_4.

Table 2. Data obtained from weight loss measurements for austenitic stainless steel in 3 M H_2SO_4 in presence of specific concentrations of the TTD at 360 h.

Sample	Corrosion rate (mm/y)	Inhibitor concentration (%)	Inhibitor efficiency (%)	Weight loss (mg)
A	23.88627	0	0	5.380
B	0.370781	0.125	98.23	0.095
C	0.212242	0.25	98.94	0.057
D	0.244253	0.375	98.81	0.064
E	0.329142	0.5	98.46	0.083
F	0.286217	0.625	98.57	0.077
G	0.416692	0.75	97.88	0.114

Open Circuit Potential measurements

A double electrode corrosion cell with an Ag/AgCl electrode as the reference electrode was used to measure the OCP Autolab PGSTAT 30 ECO CHIMIE potentiostat. Embedded sample electrodes with bare facial area of 254 mm^2 were fully and separately immersed in 200 mL of the acid media at specific concentrations of TTD for a total of 288 h. The corrosion potential of each of the sample electrodes was measured every 48 h. Plots of potential E (mV) versus immersion time T (h) (Fig. 6) for the acid solutions media obtained the tabulated data in Table 3.

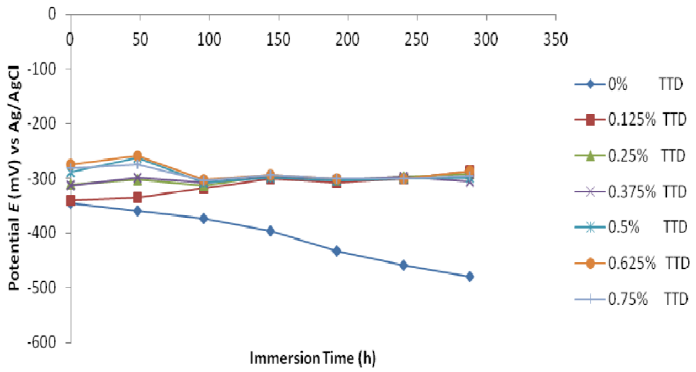

Figure 6. Variation of potential with immersion time for potential measurements in 3 M H_2SO_4.

Table 3. Data obtained from potential measurements for austenitic stainless steel in 3 M H_2SO_4 in presence of specific concentrations of the TTD.

TTD concentration / Exposure time (h)	0%	0.125%	0.25%	0.375%	0.5%	0.625%	0.75%
0	-345	-341	-310	-312	-289	-275	-281
48	-359	-335	-303	-298	-262	-259	-275
96	-374	-318	-313	-308	-307	-303	-304
144	-396	-300	-296	-297	-298	-293	-293
192	-433	-308	-303	-302	-304	-301	-301
240	-458	-300	-297	-297	-300	-301	-301
288	-479	-286	-291	-305	-299	-287	-295

Linear polarization resistance

Linear polarization was done using an Autolab PGSTAT 30 ECO CHIMIE potentiostat with the aid of embedded cylindrical samples with a facial area of 254 mm^2, and an electrode cell containing 200 mL of electrolyte at 25 ^oC, with and without TTD. A graphite rod was used as the ancillary electrode and Ag/AgCl was the reference electrode. The analyses were done from -1.5 V against OCP to +1.5 mV against OCP at a scan rate of 0.00166 V/s. The corrosion current density (i_{cr}) and corrosion potential (E_{cr}) were calculated from the Tafel plots of potential against the logarithm of current. The corrosion rate (R), the amount of surface coverage (θ) and the percentage inhibition efficiency ($\%IE$) were determined from the relationship

$$R = (0.00327 \text{ x } i_{corr} \text{ x } eq.wt/D) \quad (4)$$

where i_{corr} is the current density in uA/cm^2, D is the density in g/cm^3; $eq.wt$ is the specimen equivalent weight in grams.

The percentage inhibition efficiency (%IE) was determined from the equation below.

$$\%IE = 1 - (R_2/R_1) \text{ x } 100 \quad (5)$$

where R_1 and R_2 are are the corrosion rate with and without TTD, respectively.

Scanning Electron Microscopy characterization (SEM)

The topography and surface morphology of the steel before and after the experimental tests was studied after weight-loss analysis with the aid of Jeol JSM - 7600F UHR Analytical FEG SEM for which SEM micrographs were recorded.

X-Ray Diffraction analysis

X-ray diffraction (XRD) patterns of the film formed on the metal surface without TTD addition was analyzed using a Bruker AXS D2 phaser desktop powder diffractometer with monochromatic Cu Kα radiation produced at 30 kV and 10 mA, with a step size of 0.03^o 2θ. The measurement program is the general scan xcelerator. Analysis of the steel sample inhibited with TTD was done with a

PANalytical X'Pert Pro powder diffractometer with X'Celerator detector and variable divergence- and receiving slits with Fe filtered Co-Kα radiation. The phases were identified using X'Pert Highscore plus software.

Statistical analysis

Two-factor single level ANOVA test (*F* - test) was employed to investigate the statistical significance of the inhibitor concentration and exposure time on the performance of TTD acid solution.

Results and discussion

Weight-loss analysis

The results obtained from weight-loss (*W*), corrosion rate (*R*) and the percentage inhibition efficiency (*%IE*) are tabulated in Table 2. The corrosion rates decreased abruptly in the acid solution. Figs. 2, 3 and 4 show the graphical illustration of weight-loss, corrosion rate and percentage inhibition efficiency against exposure time at specific TTD concentrations, while Fig. 5 shows the graphical illustration of *%IE* against TTD concentration. The curves obtained show high values of *%IE* upon addition of TTD at all concentrations evaluated. The inhibition efficiency is the result of the electrochemical reactions taking place between the charged inhibitor molecules and anions of the acid solution at the metal solution interface. The steel surface is strongly protected due to the strong adsorption and protective covering of TTD. As a result of the influence of TTD on the redox electrochemical process TTD precipitates adhere to the metal samples through the exposure period inhibiting the diffusion of Cl^-/SO_4^{2-} to the metal surface, while simultaneously inhibiting the diffusion of metallic ions into the solution.

Open Circuit Potential measurements

The open-circuit potential value of the specimen electrodes was observed for a total of 288 h in the acid chloride solutions as shown in Table 3. Fig. 6 shows the plots of variation of OCP against exposure time in the acid solutions respectively in the absence and presence of specific concentrations of TTD inhibitor. A continuous potential displacement towards negative values was observed in 0% TTD in the sulphuric acid chloride media during the immersion hours due to anodic dissolution of the steel specimen. At (0.125% - 0.75%) TTD there is an instantaneous shift in corrosion potentials, positive potentials, due to the instantaneous inhibiting action of TTD. This is due to the formation of crystalline precipitates of TTD in the test solution which strongly adheres to the steel through chemisorption mechanism. The precipitates form a solid compact barrier which effectively prevents diffusion of corrosive anions unto the steel. The presence of heterocyclic atoms makes possible for charge transfer with the vacant D-orbitals of iron through electrophilic substitution. After 0% TTD, the average potential value at 288 h of exposure is -294 mV. This value is well below the potential at which corrosion occurs. It is well within passivation potentials for stainless steel. The corrosion risk is at the minimum due to the instantaneous

action of the cationic species of the TTD ions which inhibit the dissolution of the steel electrode. In H_2SO_4 competitive adsorption between the corrosive ions exists which serves to partially delay their transportation to the metal oxide interface; this in effect delays the breakdown of the passive film and aids the inhibitive action of TTD.

Polarization studies

Fig. 7a and b show the polarization plot of the stainless steel in absence and presence of TTD at specific concentrations in 3 M H_2SO_4. The corrosion rate reduced drastically in acid solutions but the electrochemical parameters varied differentially from 0% concentration. This shows that TTD significantly alters the electrochemical process responsible for corrosion. In addition, changes in the cathodic and anodic Tafel constants in the presence of TTD in contrast with the control concentration signify the suppression of redox reactions associated with the corrosion process by the surface blocking effect of the inhibitor. The inhibitive action of the inhibitor is related to its adsorption and formation of a compact barrier film on the metal electrode surface. This is further proven from the values of corrosion current and corrosion current density in comparison to the values of the control concentration.

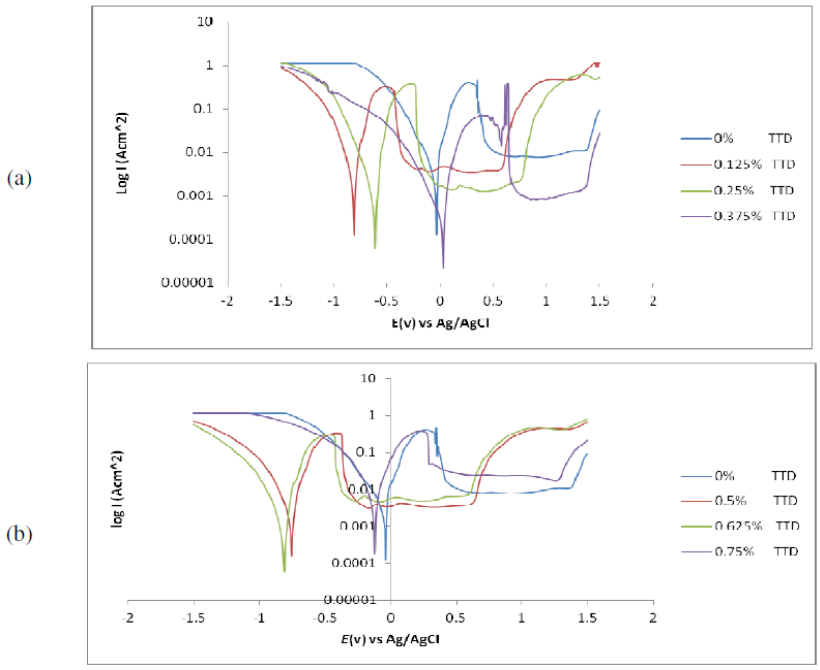

Figure 7. Comparison plot of cathodic and anodic polarization scans for austenitic stainless steel in 3 M H_2SO_4 solution in the absence and presence of specific concentrations of TTD. (a) 0% -0.375% TTD; (b) 0.5% - 0.75% TTD.

The electrochemical variables such as, corrosion potential (E_{corr}), corrosion current (i_{corr}), corrosion current density (j_{corr}), cathodic Tafel constant (bc), anodic Tafel constant (ba), surface coverage (θ) and percentage inhibition efficiency ($\%IE$) were calculated and are given in Table 4. The corrosion current density (I_{corr}) and corrosion potential (E_{corr}) were determined by the intersection of the

extrapolated anodic and cathodic Tafel lines. *%IE* (Fig. 8) was calculated from the corrosion rates obtained according to equation 6.

$$\%IE = (R_1 - R_2/R_1)\ \% \qquad (6)$$

Table 4. Data obtained from polarization resistance measurements for austenitic stainless steel in 3 M H_2SO_4 at specific concentrations of TTD.

Sample	Inhibitor concentration (%)	*ba* (V/dec)	*bc* (V/dec)	Ecorr, obs (V)	j_{corr} (A/cm²)	i_{corr} (A)	Corrosion rate (mm/yr)	Polarization resistance *Rp* (Ω)	Inhibition efficiency (%)
A	0	0.364	0.242	0.343	9.35E-03	2.38E-02	9.602	1.61	0
B	0.125	0.079	0.150	0.340	1.03E-03	2.62E-03	1.057	1.97	88.99
C	0.25	0.029	0.074	0.326	1.03E-04	2.61E-04	1.053	3.52	89.03
D	0.375	0.191	0.078	0.282	1.20E-04	3.05E-04	1.233	2.12	87.16
E	0.5	0.157	0.113	0.332	1.20E-03	3.05E-03	1.233	2.52	87.16
F	0.625	0.033	0.082	0.336	1.38E-04	3.51E-04	1.419	3.37	85.22
G	0.75	0.089	0.091	0.332	1.18E-03	3.01E-03	1.214	1.17	87.36

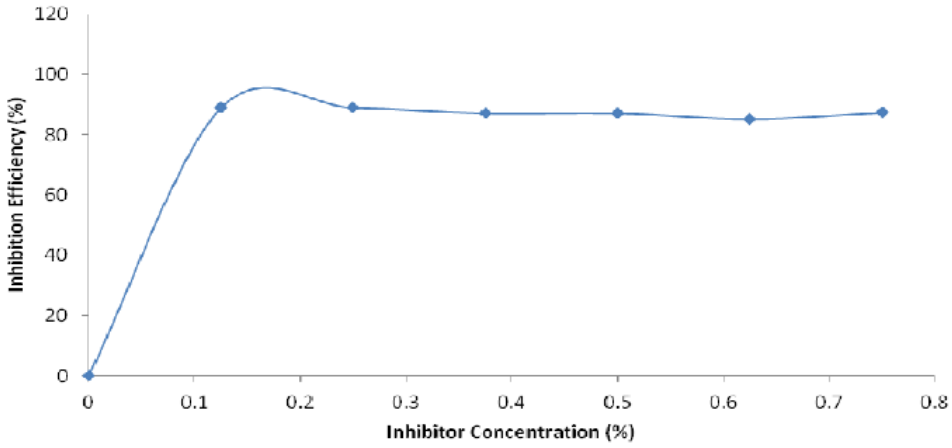

Figure 8. Relationship between *%IE* and inhibitor concentration for polarization test in 3 M H_2SO_4.

TTD appeared to act as a cathodic type inhibitor in the acid solutions as shown in the displacement of E_{corr} values in Table 4. The values of E_{corr} shifted to the less noble direction at all TTD concentrations in test solutions, an indication of its tendency to inhibit the cathodic reactions of the corrosion process. In H_2SO_4 the maximum displacement of E_{corr} value is -61 mV in the cathodic direction, thus the inhibitor is theoretically mixed but overwhelmingly a cathodic type, as shown in the E_{corr} values in Table 4. The inhibition mechanism is due to surface kinetic process which inevitably results in diffusion control. The corrosion rate is reduced without a significant change in the corrosion potential. The vacillating values of *bc* (Fig. 7) also indicate that the mechanism of proton discharge reaction changes by addition of the TTD to the acidic chloride media. The linear polarization potential values in H_2SO_4 differ significantly due to the strong influence of TTD on the passivation and repassivation characteristics of the steel which is evident on the corrosion rate and later potentiostatic study.

Mechanism of inhibition

The corrosion inhibition mechanism of TTD can be explained through the molecular adsorption phenomenon. It can be deduced from TTD molecular structure that TTD absorbs and strongly adhere onto the metal surface through π electrons of its aromatic rings (Fig.1), lone pairs of nitrogen, sulphur and oxygen electrons and as a protonated species in the acid solution. The functional group of this compound is responsible for the adsorption process, and the strength of adsorption is determined by the electron density and ionization potential of the functional group [16-18]. In the acid solutions TTD protonates and becomes positively charged but it's difficult for the positively charged inhibitor molecule to approach the positively charged metal (through electrochemical dissociation) surface because of the electrostatic repulsion between it and the stainless steel surface due to its positive charge. SO^{-2}_4/Cl^- ions are first adsorbed onto the positively charged metal surface. Then the inhibitor molecules get adsorb through electrostatic interactions between the negatively charged metal surface and positively charged TTD cations. The cationic TTD molecules are adsorbed through their multipolar centers on to the steel surface forming a protective layer (white precipitates) [19-22].

Generally, physical adsorption precedes chemisorption interaction mechanism. When more TTD adsorbs on the stainless steel surface, electrostatic interaction also takes place by partial transference of electrons from the pi-electrons of TTD ring to the metal surface. Retroactively TTD cations may also accept electrons from the metallic surface for electrochemical equilibrium from 3*d*- orbital electrons of Fe atoms to the 3*d*-vacant orbital of nitrogen and sulphur atoms [23]. Adsorption of TTD is physicochemical from the thermodynamic values (discussed later). This confirms the simultaneous process of electrostatic interaction and charge transfer mechanisms occurs in the adsorption process of TTD on the stainless steel surface. The cationic forms of TTD are adsorbed directly on the cathodic sites in competition with the protonated hydrogen atoms thereby inhibiting hydrogen evolution. This is responsible for the observed cathodic inhibiting effect of TTD [24, 25]. Accordingly, the adsorption of TTD molecules can be regarded as a substitutional electrochemical reaction mechanism of TTD and water molecules at the metal solution interface due to its hydrophobic attributes. TTD displaces water molecules from the metal surface, and interacts with the redox process thereby obstructing the diffusion of water molecules and corrosive anions to the surface. Adsorption of TTD molecule occurs because the electrostatic attraction between the metal surface and TTD is much greater than that between the metal surface and water molecules, thus they are dislodge competitively [26-28]. The differential values of the cathodic Tafel slope in H_2SO_4 indicate that the oxygen reduction reaction, one of the main cathodic processes here, is not under activation control, and that addition of TTD does modify its mechanism.

Scanning Electron Microscopy analysis

The SEM images of the stainless steel surface before immersion in the acid media and after 360 h of immersion with and without TTD are given in Fig. 9(a-c), respectively. Fig. 9a shows the steel sample before immersion: the lined surface and serrated edges are due to cutting during preparation. Fig. 9b shows the steel surfaces after 360 h of immersion in 3 M H_2SO_4 without TTD, while Fig. 9c shows the steel surface in the acid media with TTD at maximum concentration.

Fig. 9b reveals a rough surface with large pits and cracks along the grain boundary at high magnification. The pit contains an unusual high content of sulphur and chloride atoms, proving them responsible for pit formation. The corrosion attack of the steel specimen is most probably a result of competitive adsorption/diffusion, whereby the anions move into the metal/liquid interface of the steel surface and displace the species. They initiate and enhance the rate of iron diffusion into the solution. This is responsible for the uneven topography on the steel most especially at sites with flaws and inclusions. The corrosion is also observed to occur along the grain boundary due to its susceptibility to corrosion. These pits are surrounded by iron oxide layer which almost fully covers the stainless steel surface, revealing that pit formation under these conditions occurs continuously during the exposure period, while iron oxide builds up over the surface. Most pits often grow with a porous cover which makes visual detection extremely difficult [29, 30]. Fig. 9c contrasts the appearance in Fig. 9b due to the accumulation of TTD precipitates on the specimen surface which effectively seals it against further corrosion.

XRD analysis

The X-ray diffraction (XRD) patterns of the stainless steel surfaces after immersion in 3 M H_2SO_4 solutions with and without the addition of TTD are shown in Fig. 10 and Table 5, respectively. The peak values at 2θ for the steel specimen in the absence of TTD in H_2SO_4 solutions showed the presence of phase compounds, i.e., corrosion products on the steel surface. The peak values at 2θ = 89.4° and 111.2° for the steel after immersion in 3 M H_2SO_4 (Fig. 10) correspond to iron (ii, iii) oxide (Fe_3O_4) present on the surface quantitatively. Observation of the peak values (Fig. 11) on the surface of the steel after immersion in the acid solutions with TTD revealed the absence of phase compounds, hence corrosion products due to effective TTD inhibition.

Adsorption isotherm

The mechanism of corrosion inhibition can be further proven from adsorption behavior of TTD on the metal surface as it gives understanding to the inhibition mechanism in electrochemical reactions. Strong adsorption bond/high surface coverage induced by chemical activity must be the basis of effective inhibition between TTD molecules and the metal surface compared to the interaction between TTD and water molecules. The adsorption of TTD at the metal/solution interface is due to the formation of either electrostatic or covalent bonding between ionized molecules or the metal surface atoms. Langmuir adsorption

isotherm was applied to describe the adsorption mechanism for TTD compounds in 3 M H_2SO_4.

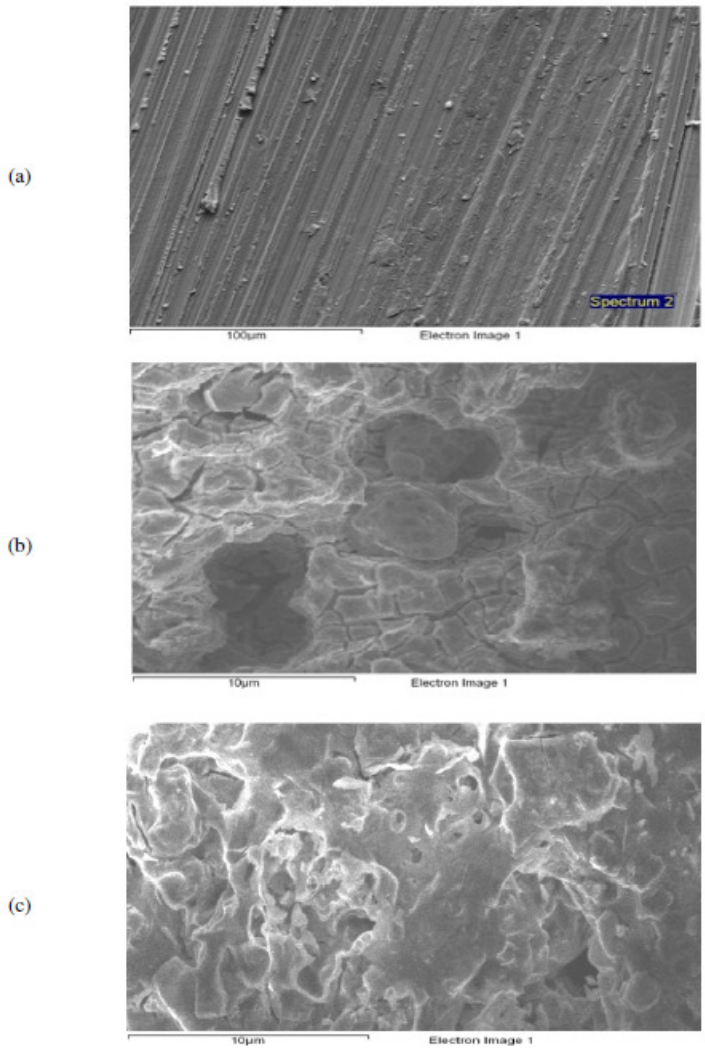

Figure 9. SEM micrographs of: a) austenitic stainless steel, b) austenitic stainless steel in 3 M H_2SO_4 and c) austenitic stainless steel in 3 M H_2SO_4 with TTD.

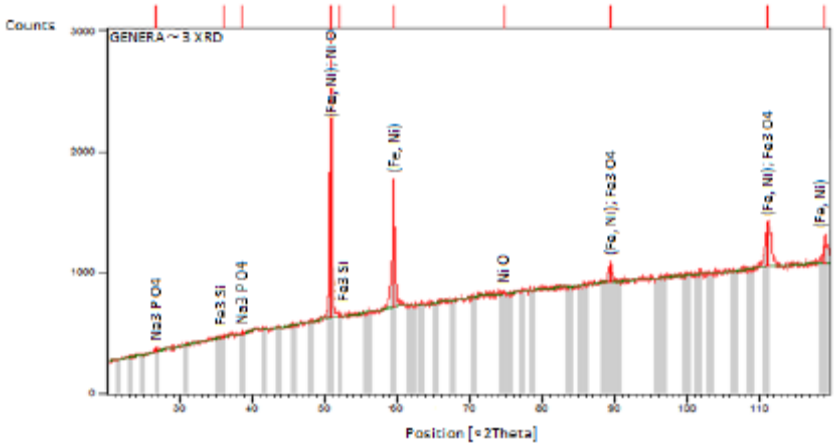

Figure 10. XRD pattern of the surface film formed on austenitic stainless steel after immersion in the absence of TTD in 3 M H_2SO_4.

Table 5. Identified patterns list for XRD analysis of austenitic stainless steel in 3 M H_2SO_4 without TTD.

Ref. code	Score	Compound name	Displacement [°2Theta]	Scale factor	Chemical formula
00-047-1417	61	Taenite, syn	-0.095	0.974	(Fe , Ni)
00-065-3005	41	Iron silicon	-0.993	0.01	Fe_3 Si
00-008-0087	38	Iron oxide	0.173	0.078	Fe_3 O_4
01-084-0195	25	Sodium phosphate	-0.723	0.016	Na_3 P O_4
01-089-5881	21	Nickel oxide	-0.018	0.341	Ni O

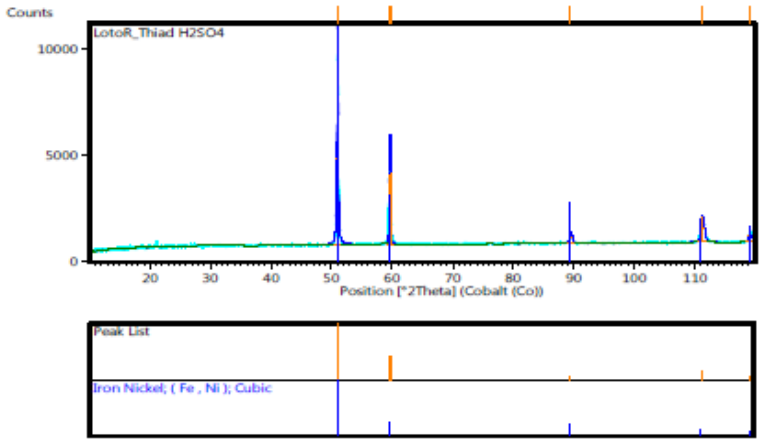

Figure 11. XRD pattern of the surface film formed on austenitic stainless steel after immersion in the presence of TTD in 3 M H_2SO_4.

All of these isotherms are of the general form

$$f(\theta, x) \exp(-2a\theta) = K_{ads}C \qquad (8)$$

where $f(\theta, x)$ is the configurational factor which depends upon the physical model and assumption underlying the derivative of the isotherm, θ is the surface coverage, C is the inhibitor concentration, x is the size ration, 'a' is the molecular interaction parameter and K_{ads} is the equilibrium constant of the adsorption process.

The general equation for Langmuir isotherm is,

$$\theta / 1 - \theta = K_{ads}C \qquad (9)$$

and rearranging gives

$$K_{ads}C = (\theta / 1 + K_{ads}\theta) \qquad (10)$$

θ is the degree of coverage on the metal surface, C is the inhibitor concentration in the electrolyte, and K_{ads} is the equilibrium constant of the adsorption process. The plots of C/θ versus the inhibitor concentration C were linear (Fig. 12), indicating Langmuir adsorption.

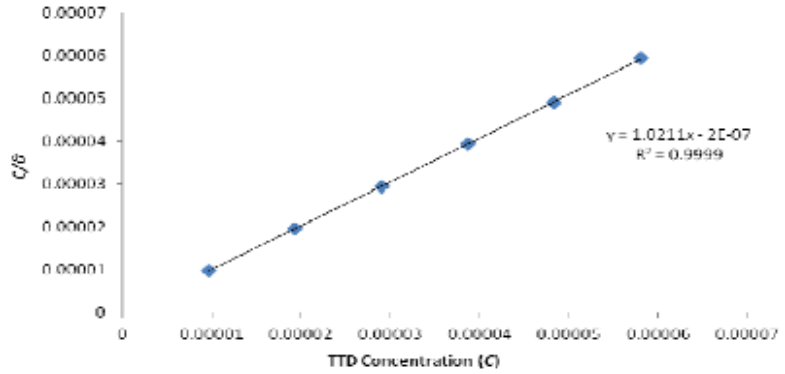

Figure 12. Relationship between C/θ and the inhibitor concentration (C) in 3 M H_2SO_4.

The divergence of the slopes from unity in Fig. 12 is as a result of the electrochemical interaction among the adsorbed TTD ions on the metal surface and changes in the values of Gibbs free energy as the surface coverage increases. This was not taken into cognizance when the Langmuir equation was being formulated. Langmuir isotherm states the following:

(i) The metal surface has a definite proportion of adsorption sites with one adsorbate.

(ii) Gibbs free energy of adsorption has the same value for the sites, independent of the value of surface coverage.

(iii) There is no evidence of lateral interaction between the adsorbed inhibitor molecules [31].

The fitted lines from the Langmuir equation show values less than unity for the slopes. This suggests a slight deviation from ideal conditions assumed in the equation.

Thermodynamics of the corrosion process

The values (Table 6) of the apparent free energy change, i.e., Gibbs free energy (ΔG_{ads}) for the adsorption process can be evaluated from the equilibrium constant of adsorption using the following equation:

$$\Delta G_{ads} = -2.303\, RT \log [55.5\, K_{ads}] \qquad (11)$$

where 55.5 is the molar concentration of water in the solution, R is the universal gas constant, T is the absolute temperature and K_{ads} is the equilibrium constant of adsorption. K_{ads} is related to surface coverage (θ) by the following the equation:

$$K_{ads}C = (\theta / 1 - \theta) \qquad (12)$$

The results presented in Table 6 provide additional proof of slight deviation from ideal condition of Langmuir model, as observed in the differential values of free energy of adsorption (ΔG_{ads}) with increase in surface coverage (θ) values. The dependence of free energy of adsorption (ΔG_{ads}) of TTD on surface coverage is ascribed to the heterogeneous characteristics of the metal surface, thus the differential adsorption energies as observed in the experimental data (Table 6). The energy of adsorption depends on factors such as micro pits, slag inclusion, elemental variations, dislocations, and cracks along the grain boundary, etc., at the metal surface. Values of ΔG_{ads} about -20 kJ/mol or below are consistent with physisorption characteristics; those of about -40 kJ/mol or above involve charge

sharing or transfer between the adsorbate and absorbent to form covalent bonds associated with chemisorption. The value of ΔG_{ads} in H_2SO_4 reflects strong adsorption of TTD to the stainless steel. The negative values of ΔG_{ads} show that TTD adsorption on the metal surface is spontaneous [32]. The values of ΔG_{ads} calculated ranges between −48.50 and −43.68 kJ mol^{-1} for TTD in H_2SO_4 solutions.

Table 6. Data obtained for the values of Gibbs free energy, surface coverage and equilibrium constant of adsorption at varying concentrations of TTD in 3 M H_2SO_4.

Inhibitor concentration (%)	Free energy of adsorption (ΔG_{ads})(KJ/mol)	Surface coverage (θ)	Equilibrium constant of adsorption (K_{ads})
0	0	0	0
0.125	-48.50	0.9823	5749202.1
0.25	-48.10	0.9894	4825437.3
0.375	-46.79	0.9881	2861338.1
0.5	-45.42	0.9846	1648834.1
0.625	-45.08	0.9857	1423463.0
0.75	-43.65	0.9788	795628.2

The results presented in Table 6 provide additional proof of slight deviation from ideal condition of Langmuir model, as observed in the differential values of free energy of adsorption (ΔG_{ads}) with increase in surface coverage (θ) values. The dependence of free energy of adsorption (ΔG_{ads}) of TTD on surface coverage is ascribed to the heterogeneous characteristics of the metal surface, thus the differential adsorption energies as observed in the experimental data (Table 6). The energy of adsorption depends on factors such as micro pits, slag inclusion, elemental variations, dislocations, and cracks along the grain boundary, etc., at the metal surface. Values of ΔG_{ads} about -20 kJ/mol or below are consistent with physisorption characteristics; those of about -40 kJ/mol or above involve charge sharing or transfer between the adsorbate and absorbent to form covalent bonds associated with chemisorption. The value of ΔG_{ads} in H_2SO_4 reflects strong adsorption of TTD to the stainless steel. The negative values of ΔG_{ads} show that TTD adsorption on the metal surface is spontaneous [32]. The values of ΔG_{ads} calculated ranges between −48.50 and −43.68 kJ mol^{-1} for TTD in H_2SO_4 solutions.

Statistical analysis

Two-factor single level experimental ANOVA test (F - test) was used to analyse the separate and combined effects of the percentage concentrations of TTD and exposure time on the inhibition efficiency of TTD in the corrosion inhibition of low carbon steels in 3 M H_2SO_4 solutions and to investigate the statistical significance of the effects. The F - test was used to examine the amount of variation within each of the samples relative to the amount of variation between the samples.

The sum of squares among columns (exposure time) was obtained with equation 13.

$$SS_c = [(\sum T^2_c/nr) - (T^2/N)\ SS_c] \quad (13)$$

Sum of squares among rows (inhibitor concentration)

$$SS_r = [(\sum T^2_r/nc) - (T^2/N)\ SS_r] \quad (14)$$

Total sum of squares

$$SS_{Total} = [\sum x^2 - (T^2/N)\ SS_{Total}] \quad (15)$$

The results using the ANOVA test are tabulated (Table 7).

Table 7. Analysis of variance (ANOVA) for inhibition efficiency of TTD inhibitor in 3 M H_2SO_4 (at 95% confidence level).

Source of variation	**Sum of squares**	**Degree of freedom**	**Mean square**	**Mean square ratio**	**Min. MSR at 95% confidence Significance F**		**F (%)**
Inhibitor concentration	12.90	5	2.58	0.25	2.71	Inhibitor concentration	83.96
Exposure time	6.27	4	1.57	0.15	2.87	Exposure time	10.46
Residual	202.56	20	10.13				
Total	221.72	29					

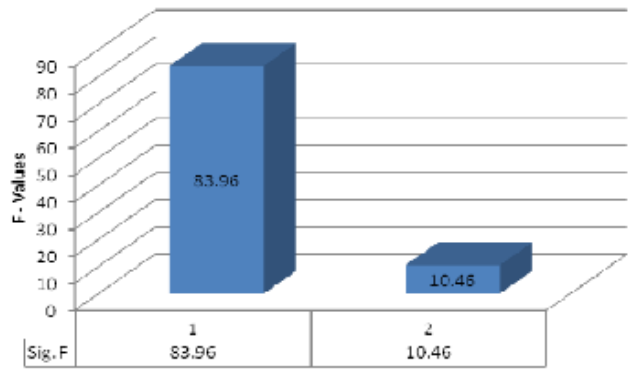

Figure 13. Influence of the inhibitor concentration and exposure time on inhibition efficiency of TTD in 3 M H_2SO_4.

The statistical analysis in 3 M H_2SO_4 was evaluated for a confidence level of 95%, i.e., a significance level of $\alpha = 0.05$. The ANOVA results (Table 7, Fig. 13) in the acid solution reveal the overwhelming influence of the inhibitor concentration on the inhibition efficiency with F - value of 0.25. These are greater than the significance factor at $\alpha = 0.05$ (level of significance or probability). The F - values of exposure time in acid solution are less significant compared to the inhibitor concentration, but greater than the significant factor hence they are statistically relevant with F - value of 0.15. The statistical influence of the inhibitor concentration in H_2SO_4 is 83.96%, while the influence of the exposure time is 10.46%. The inhibitor concentration and exposure time

are significant model terms influencing the inhibition efficiency of TTD on the corrosion of the steel specimen with greater influence from the percentage concentration of TTD.

Conclusions

2-amino, 5-ethyl- 1, 3, 4-thiadiazole (TTD) performed effective as a potent corrosion inhibiting compound. The following conclusions were deduced from the experimental investigation.

1. Application of TTD drastically reduced the corrosion rate of the stainless steel samples giving an average inhibition efficiency of 98% from weight loss analysis and 88.9% from polarization resistance technique at all concentrations studied.
2. Open circuit potential monitoring results showed corrosion potential values well below values responsible for corrosion reactions.
3. Adsorption on the steel surface obeyed the Langmuir adsorption isotherm, thus indicating that the metal surface has a definite proportion of adsorption sites with one adsorbate while the Gibbs free energy of adsorption has the same value for the sites, independent of the value of surface coverage.
4. XRD analysis showed the absence of phase compounds, i.e., corrosion products on the steel surface immersed in TTD; this contrast results obtained in the absence of TTD.

Acknowledgements

The authors express their sincere gratitude to the Department of Chemical, Metallurgical and Materials Engineering, Tshwane University of Technology, for their support and provision of research facilities.

References

1. Ashassi-Sorkhabi H, Masoumi B, Ejbari PE. J Appl Electrochem. 2009;39:1497-1501
2. Singh DDN, Singh TB, Gaur B. Corros. Sci. 1995;37:1005-1019.
3. Ashassi-Sorkhabi H, Majidi MR, Seyyedi K. Appl Surf Sci. 2004;225:176-185.
4. El-Etre AY. Corros Sci. 2003;45:2485-2495.
5. El-Etre AY. Corros Sci. 1998;40:1845-1850.
6. Airey K, Armstrong RD, Handyside T. Corros Sci. 1998;28:449-460.
7. Cohen M. Corrosion J. 1976;32:461-465.
8. Rajendran S, Apparao BV, Palaniswamy N. Anti-Corros Methods Mater. 1997;44:308-313.
9. Mansa JL, Szybalski W. Corrosion. 1952;8:381-390.
10. Morad MS. Corros Sci. 2008;50:436-448.
11. Xuehui P, Xiangbin R, Fei K, et al. Chinese J Chem Eng. 2010;18:337-345.
12. Natarajaa SE, Venkateshaa TV, Tandonb HC. Corros Sci. 2012;60:214-223.

13. Fouda AS, Ellithy AS. Corros Sci. 2009;51:868-875.
14. Naqvi I, Saleemi AR, Naveed S. Int J Electrochem Sci. 2011;6:146-161.
15. Derya LH, Kaan CE, Orhan A. Corros Sci. 2008;50:1460-1468.
16. Fouda AS, Moussa M, Taha F, et al. Corros Sci. 1986;26:719-726.
17. Singh AK, Quraishi MA. J Appl Electrochem. 2011;41:7-18.
18. Schweinsberg DP, Graeme A, Nanayakkara AGAK, et al. Corros Sci. 1988;28:33-42.
19. Obi-Egbedi NO, Obot IB. Arabian J Chem. 2013;6:211-223.
20. Ritchie IM, Bailey S, Woods R. Adv Colloid Int Sci. 1999;80:183-231.
21. Mu GN, Zhao TP, Liu MGT. Corrosion J. 1996;52:853-856.
22. Solmaz R, Kardas G, Yazici B, et al. Colloid Surf A: Physicochem Eng Asp. 2008;312:7-17.
23. Ahmed YM, AbuBakar M, AbdulAmir HK, et al. J Ind Eng Chem. 2012;18:551-555.
24. Agarwal P, Landolt D. Corros Sci. 1998;40:673-680.
25. Philippe K, Dieter L. Electrochim Acta. 2001;47:589-598.
26. Khaleda KF, El-Maghraby A. Arabian J Chem. 2014;7:319-326.
27. Quraishi MA, Sardar R. J Appl Electrochem. 2003;33:233-238.
28. Muthukumar N, Ilangovan A, Maruthamuthu S, et al. Mater Chem Phys. 2009;115:444-452.
29. Frankel GS. J Electrochem Soc. 1198;145:2186-2198.
30. Laycock NJ, White SP, Noh JS, et al. J Electrochem Soc. 1998;145:1101-1108.
31. Ashish KS, Quraishi MA. Corros Sci. 2011;53:1288-1297.
32. Hosseini MG, Mertens SFL, Arshadi MR. Corros Sci. 2003;45:1473-1489.